Research article Available online www.ijsrr.org ISSN: 2279–0543

International Journal of Scientific Research and Reviews

Oil spillage Removal using Maleic Anhydride grafted Polypropylene anchored Magnetic Cellulose Nanocomposites

V.Sasi Bremila[1] and Suresh Chandra Kumar[1*]

[1]Department of Chemistry, Scott Christian College (Autonomous), Nagercoil, affiliated to Manonmaniam Sundaranar University, Tirunelveli, Tamil Nadu, India

http://doi.org/10.37794/IJSRR.2019.8416

ABSRACT

In this study, the oil absorption capacity of maleic anhydride grafted polypropylene anchored magnetic cellulose nanocomposites (MAPP-a-MCNFs/PP) was investigated. Carboxylated cellulose nanofibrils (CCNFs) were prepared from bamboo strips. The sol-gel process using magnetite nanoparticles (Fe_3O_4 NP) and CCNFs were utilized to synthesize magnetic cellulose nanofibrils (MCNFs). Surface modification of MCNFs were done through hydrolysis–condensation reaction using 3-aminopropyltriethoxysilane (γ-APTES) coupling agent, followed by amidation with maleic anhydride grafted polypropylene (MAPP) to produce maleic anhydride grafted polypropylene anchored magnetic cellulose nanofibrils (MAPP-a-MCNFs). The MAPP-a-MCNFs/PP nanocomposite was characterized with FTIR, TGA and SEM. The nanocomposites absorb heavy crude oil fast and selectively on water surface, and the removal of the absorbed oils from the water surface was readily achieved under a magnetic field. This study proposes an economic and novel method for the large-scale preparation of superabsorbent nanocomposites, making them a promising candidate for the efficient and sustainable cleaning of oil spills.

KEYWORDS: MAPP-a-MCNFs/PP nanocomposites, oil absorption, magnetic field.

*Corresponding author

Dr. M. Suresh Chandra Kumar

Department of Chemistry

Scott Christian College (Autonomous)

Nagercoil – 629 003, Tamil Nadu, INDIA

Email: sure_chandra@yahoo.com, Mob. No - 9442258686

1. INTRODUCTION

Crude oil is a naturally occurring energy rich material.[1] When oil is explored, transported and stored, there is a risk of spillage over the seas, water bodies and land surfaces.[2] Oil spillage has enormous adverse effects on the environment due to its physical, ecological and chemical changes. The progressive change of physical and chemical properties of oil in water is referred to as "weathering".[3,4] The weathering process includes evaporation, dissolution, dispersion, photochemical oxidation, microbial degradation, and adsorption onto the suspended materials.[5,6] Hazardous chemicals are released from oil spills which has harmful effects to the marine resources and coastal environment.[7.8] So, it is essential to clean-up the oil spill immediately from the water bodies.

The methods developed to clean-up oil spills are physical methods, chemical methods and biological methods.[6] Physical methods employ barriers like sorbents, skimmers and boomers to control the spread of an oil spill.[3] However, these physical methods of cleaning are not suitable for rough sea surface, high wind velocity and waves. Chemical methods of cleaning not only block the spreading of the oil spill, but also protect the shoreline and sensitive marine habitats. But, the chemical dispersant may affect deep water corals, sea grass and marine organisms. Biological method refers to bioremediation, in which microorganisms are used to degrade and metabolize chemical substances of oil and restore environment quality.[9] Even though, bioremediation is a cheap, sustainable method, is benign to the environment. In-situ burning of oil spill is successful in open water body, i.e. ocean, where there is no ship movement.[10] Among the existing techniques, physical method using sorbents is considered to be the most efficient technique available for removal of oil and polycyclic aromatic hydrocarbons (PAHs) from water.[11] Oil sorbents are more popular owing to simplicity, low cost of operation and ready availablity.[12] Other methods have negative impact on the environment. Even though diverse methods are available to clean-up oil spills, different nations adapt different methods of clean-up technology depending upon the individual circumstances of the spill (location, type of oil, and quantity of oil) and also unpredictable variable like weather. In general, two or more methods are combined to achieve effective clean-up of oil spills.[13]

Recently, several research groups have invested a lot of effort for the synthesis of materials having simultaneous hydrophobic and oleophilic nature.[14-18] Careful manipulation of structural and surface properties of magnetic materials demonstrated superhydrophobic/superoleophilic properties which can be used for simultaneous oil adsorption and water repulsion. For example, superhydrophobic

and superoleophilic three-dimensionally macroporous Fe/C nanocomposites have been fabricated to selectively absorb oil.[19] Qing Zhu et. al. [20] fabricated superhydrophobic core–shell Fe_2O_3@C nanoparticles to remove oil from water. The specific area of Fe_2O_3@C nanoparticle was 94.04 m^2/g, and the water contact angle was 163°. Ting Lü et. al. [21] prepared chitosan coated iron oxide nanoparticles by grafting chitosan onto Fe_3O_4 followed by silica coating using 3-aminopropyltriethoxysilane (APTES) which could separate 90% of oil from diesel-in-water emulsion. The magnetic nanomaterials have unsinkable properties to contact the oil fully and obtain greatest removal efficiency. Polymer coated magnetic nanoparticles are also having low density so that they can be easily collected after adsorption.[22] Due to the ferromagnetic properties of Fe_3O_4 nanoparticles, the magnetic materials could be collected easily and quickly after adsorption by an external magnetic field.[23] According to recent studies, magnetic oil adsorbents can be reused several times. [24]

In this study, we have synthesized magnetic cellulose nanofibrils by the sol-gel process. Surface modification of magnetic cellulose nanofibrils (MCNFs) were done through hydrolysis–condensation reaction using 3-aminopropyltriethoxysilane coupling agent, followed by amidation of amine groups of silane with maleic anhydride grafted polypropylene (MAPP) to produce an maleic anhydride grafted polypropylene anchored magnetic cellulose nanofibrils (MAPP-a-MCNFs). This strategy will increase interfacial adhesions between the MAPP-a-MCNFs and the PP matrix. Polypropylene coated Fe_3O_4@cellulose nanocomposites remain sterically stable even in complex environments and show little hazard.

2. MATERIALS AND METHODS

2.1 Materials

Bamboo strips were purchased from local market at Nagercoil, Tamil Nadu. 3-aminopropyltriethoxysilane (γ-APTES), boiling point = 217 °C, density = 0.946 $g.cm^{-3}$, M_w = 221.3, relative density = 0.95 @ 25 °C and maleic anhydride grafted polypropylene (MAPP), Mw = 9100 by GPC, maleic anhydride = 8 to 10% were purchased from Aldrich, USA. Isotactic polypropylene (REPOL HO20EG), density – 0.905 g/cm^3, melting point – 160-170 °C, melt flow index – 2.0 g/10 min., heat deflection temperature – 104 °C was obtained from Reliance Industries Ltd, India. Analytical grade $FeCl_3 \cdot 6H_2O$, $Fe_2SO_4 \cdot 7H_2O$, KOH, toluene, acetone, ethanol, xylene, were used. Sea water was collected from Arabian Sea at Colachel, Kanyakumari District, Tamil Nadu, India.

2.2 Methods of Preparation

Preparation of cellulose nanofibrils from Bamboo

Preparation of micro crystalline cellulose fibers was carried out by the method already reported. [25] In short, bamboo strips were washed with water to remove solid impurities and dried at 50 ^{o}C for 48 h. Dried bamboo strips were grinded using a mini crusher and sieved using the 75 µm and 150 µm sieves. The larger and unwanted particles were discarded during the sieving process from bamboo powder. Bamboo powder was extracted with ethanol and toluene at 110 ^{o}C for 6 h to remove extractives and waxes. The lignin and hemicellulose of bamboo were isolated from the lignocellulose of bamboo by treating with KOH at a temperature of 80 ^{o}C for 4 h. The undissolved micro crystalline cellulose was purified to eliminate the phenolic component by using NaOCl and H_2O_2 for bleaching at a temperature of 30 ^{o}C for 3 h. Micro crystalline cellulose fibers was washed with deionized water until it reached the pH of 7, filtered and dried.

Micro crystalline cellulose fibers (15 g) and tungsten carbide grinding balls (6–10 mm in diameter) were taken in a 500 ml hardened stainless steel grinding bowl at the volume ratio of 1:2 in a pulverisette 6" planetary monomill (Fritsch GmbH, Germany). Grinding operations were carried out in dry mode for 12 h. Temperature of the grinding bowl was maintained at 30 ^{o}C by cold water circulation. Cellulose nanofibrils (CNFs) were oven dried at 100 ^{0}C for 12 h, cooled and kept in a dessicator.

Preparation of carboxylated cellulose nanofibrils

10 g of cellulose nanofibrils and 1000 ml 1 M aqueous solution of ammonium persulphate (APS) were taken in a 2 L R.B flask. Hydrolysis of CNFs was carried out at 80 ^{o}C for 4 h with constant stirring. The suspension was diluted with cold distilled water to stop the reaction, and then centrifuged for 10 min. at 12,000 rpm. The centrifugation was carried out several times until a constant pH (pH- 4) was attained. Carboxylated cellulose nanofibrils (CCNFs) was obtained by freeze drying and kept in a dessicator.

Synthesis of magnetic cellulose nanofibrils

Magnetite nanoparticles (Fe_3O_4 NP) were synthesized by co-precipitation method.[26] Fe_2SO_4·7H2O (5.56 g) and $FeCl_3$·$6H_2O$ (10.8 g) were dissolved in 200 mL of deionized water. 120 mL of 25% (v/v) aqueous ammonia was added to it in drops with vigorous stirring at 25 °C. The suspension was incubated at 85 °C for 30 min. under N_2 atmosphere and cooled to room temperature.

The black coloured Fe_3O_4 nanoparticles were centrifuged, washed with distilled water and absolute ethanol. The black solid were dried in a vacuum oven at 60 °C for 4 h.

Magnetic cellulose nanofibrils were synthesized by the sol-gel process. 3 g of Fe_3O_4 nanoparticles were dispersed in a mixture of 120 ml of ethanol and 40 ml of water, sonicated for 15 min. at 150 rpm in 37 °C. 27 g of carboxylated cellulose nanofibrils (CCNFs) were dissolved in 400 ml ethanol. Then the dispersion of magnetic nanoparticle was added slowly to the carboxylated cellulose nanofibrils solution and heated to 45 °C for 12 h at 180 rpm. Afterward Fe_3O_4-cellulose nanofibrils were collected by external magnetic field and washed with distilled water, ethanol and hexane and dried.

Preparation of PP coated Fe_3O_4@cellulose Nanocomposites

A solution of 3-aminopropyltriethoxysilane (γ- APTES) was prepared by adding 9 g of γ-APTES to 250 mL of a methanol–water mixture (9/1; v/v) and stirred for 30 min. 3 g of Fe_3O_4-cellulose nanofibrils were added to the γ-APTES solution and stirred for 3 h. The silane-treated magnetic cellulose nanofibrils were centrifuged, washed with deionised water and dried in vacuum at 60 °C. Maleic anhydride grafted polypropylene (MAPP) was dissolved in xylene at 120 °C. Silane-treated magnetic cellulose nanofibrils were added to the xylene solution and stirred for 6 h at 120 °C. The maleic anhydride grafted polypropylene anchored magnetic cellulose nanofibrils (MAPP-a-MCNFs) was centrifuged, washed with xylene and dried in vacuum at 80 °C for 3 days to evaporate the solvent completely.

Isotactic Polypropylene (20 g) was dissolved in xylene (200 mL) and refluxed at 140 ^oC for 2 h. Calculated amount of maleic anhydride grafted polypropylene anchored magnetic cellulose nanofibrils (MAPP-a-MCNFs) was injected into the solution and refluxed for 3 h. The MAPP-a-MCNFs/PP nanocomposites solution was cooled down to around 90 ^oC and then poured onto a large glass plate to allow the solvent evaporation overnight. The powder-like products were collected and dried in a vacuum oven at room temperature overnight.

Oil sample

The heavy crude oil used through all experiments were procured from Oil Natural Gas Commission, Ahmadabad asset, India has density 997 Kg/m^3 at 20 ^oC, API gravity 19.32 (ASTM D 28) and acid number 1.726 g KOH/g oil. Since the experiments were carried out at room temperature (25 ^oC) it is expected for the crude oil to be slightly less dense. However, the low boiling fractions of

crude oil evaporates rapidly after a spill and oil viscosity increase often before significant clean-up operations can take place. Thus, in order to simulate this situation of oil spill and to minimize experimental variation, the crude oils were held in thin layers in trays for one and seven days in open air. In the case of one days weathered oil (1 DWO), this treatment causes a weight loss of 15.58 % while for seven days weathered oil (7 DWO) the weight loss was 37.28 %.

3 CHARACTERIZATION OF MATERIALS

The FT-IR spectra of the samples were recorded on a Shimadzu 1800S spectrophotometer using a KBr disc. The samples were scanned from 400 to 4000 cm^{-1}. Thermal stability was determined on a thermogravimetric analyzer (NETZSCH TG 209) between 0 and 700 ^{o}C at a rate of 10 ^{o}C per minute under nitrogen atmosphere. Morphology and microstructural characterization were performed using a field emission scanning electron microscope (Nova NanoSEM NPE 206) at an accelerated voltage of 8 kV.

3.1 Oil Absorptivity

20 ml of crude oil was poured into a 200 ml beaker containing 80 ml of sea water (pH = 7.2) to form artificial oil-water bath. 0.5 g of the MAPP-a-MCNFs/PP nanocomposites were scattered on the surface of oil-water mixture. The beaker containing the oil sample and the sea water was mounted in a shaker which was shaken for 5 min at 105 cycle /min. The bath temperature was kept constant at 25 ± 1°C using thermostatic water bath. Excess amount of crude oil in the beaker was chosen so that there was still plenty of oil remaining in the beaker after completion of the absorption test. After 5 min, the nanocomposites soaked with oil were separated from the water surface using a cylindrical permanent magnet and weighted by an electronic balance.

The oil-absorption capacity of the nanocomposites was calculated by the formula:

$$k = (m_2 - m_1) / (m_1)$$

where k is the sorption capacity (g/g), $m_1$and m_2 are the weight of the materials before and after oil absorbance, respectively.

Weight of oil absorbed: $m = m_2 - m_1$

All the absorption experiments were repeated for three times. The absorbed oil was removed from the surfaces of the nanocomposites by ultrasonically washing in ethanol for 5 min. After being dried in a vacuum oven, the nanocomposites were reused to separate the water and oil mixture.

4. RESULTS AND DISCUSSION

4.1 FTIR Spectroscopic Analysis

Fig. 1 shows the FT-IR spectrum of carboxylated cellulose nanofibrils. It was observed that O-H stretching vibration at 3440 cm^{-1}, C–H stretching vibration at 2895 cm^{-1}, O-C-H in-plane bending vibration at 1425 cm^{-1}, C-H deformation vibration at 1375 cm^{-1} and β-glycosidic linkages between glucopyranose units at 1013 cm^{-1}. However, C=O stretching vibration at 1735 cm^{-1} indicated the carboxylation of cellulose by APS.[27] FTIR spectrum of Fe_3O_4 NP is given in Fig. 2. The three peaks at 640, 563, and 440 cm^{-1} represent the Fe-O absorption, and the peak at 1635 cm^{-1} represents the O-H deformation vibration. A band at 3448 cm^{-1} is attributed to Fe-OH stretching vibration.[28]. Fig. 3 presents FTIR spectrum of maleic anhydride grafted polypropylene (MAPP). It was observed that C-CH_3 stretching and CH_2 rocking vibrations at 840 cm^{-1}, C-C stretching and CH_3 rocking vibrations at 974 cm^{-1}, C-H bending and CH_2 wagging vibrations at 999 cm^{-1}, CH_3 bending vibration at 1379 cm^{-1} and C-H asymmetric stretching vibrations at 2921 cm^{-1}. The FTIR spectrum of MAPP shows bands at 1710, 1722 and 1746 cm^{-1}, which can be assigned to the C=O stretching vibration of cyclic anhydride groups and carboxylic acid respectively. Carboxylic acid is present because the grafted anhydride absorbs moisture from the environment and undergoes hydrolysis.[29]

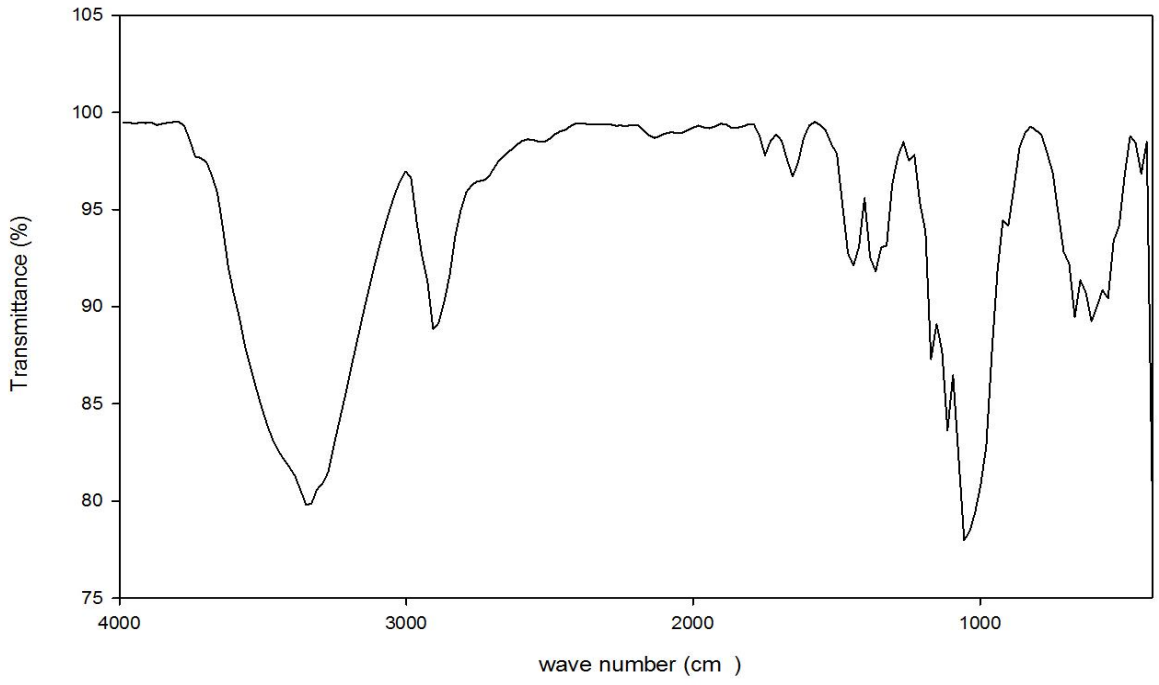

Figure1 FTIR spectra of carboxylated cellulose nanofibrils

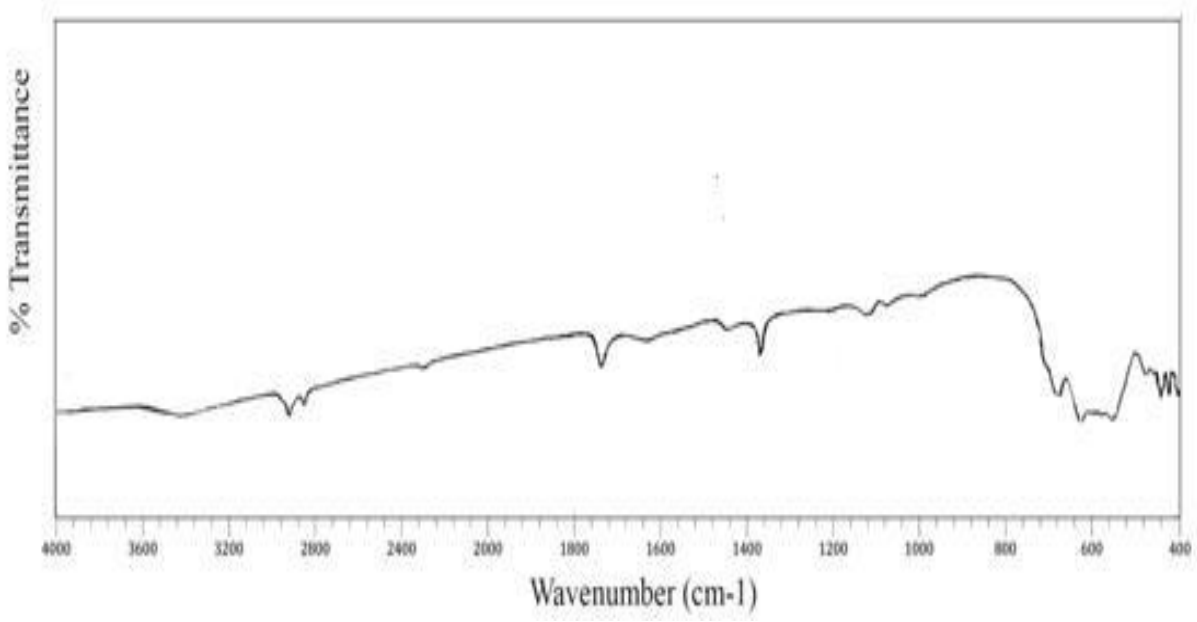

Figure 2 FTIR spectra of Fe_3O_4 NPs

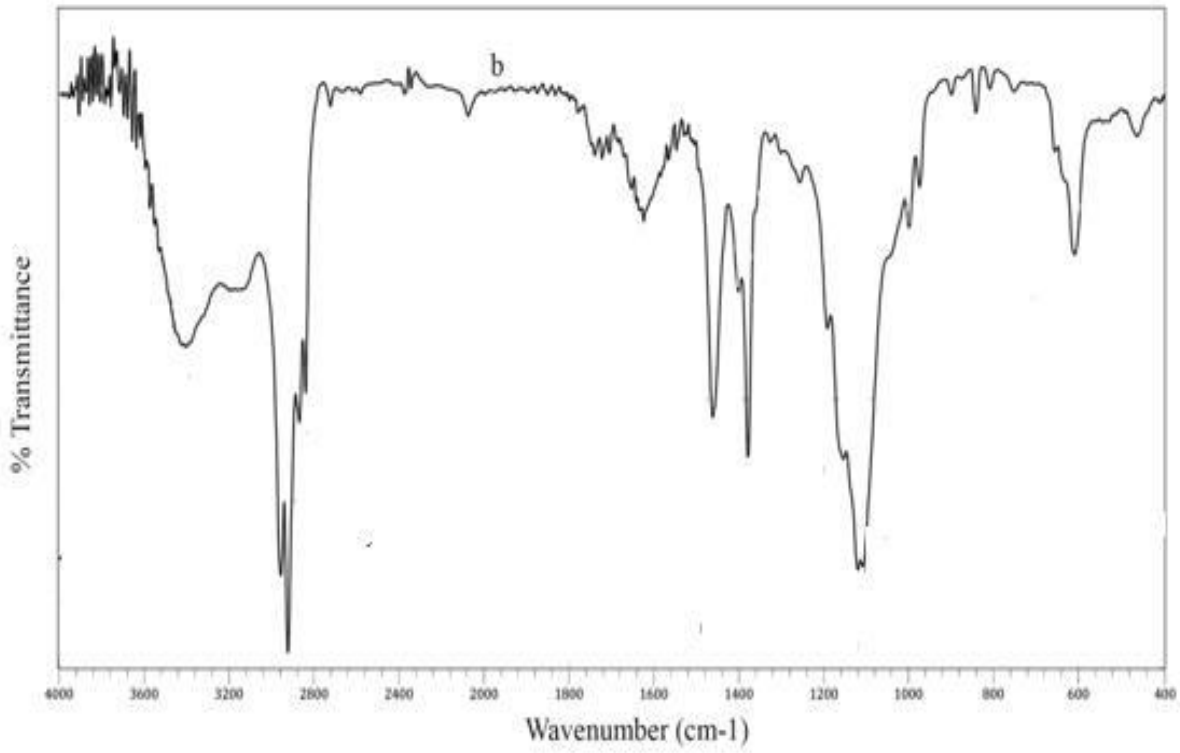

Figure 3 FTIR spectra of MAPP

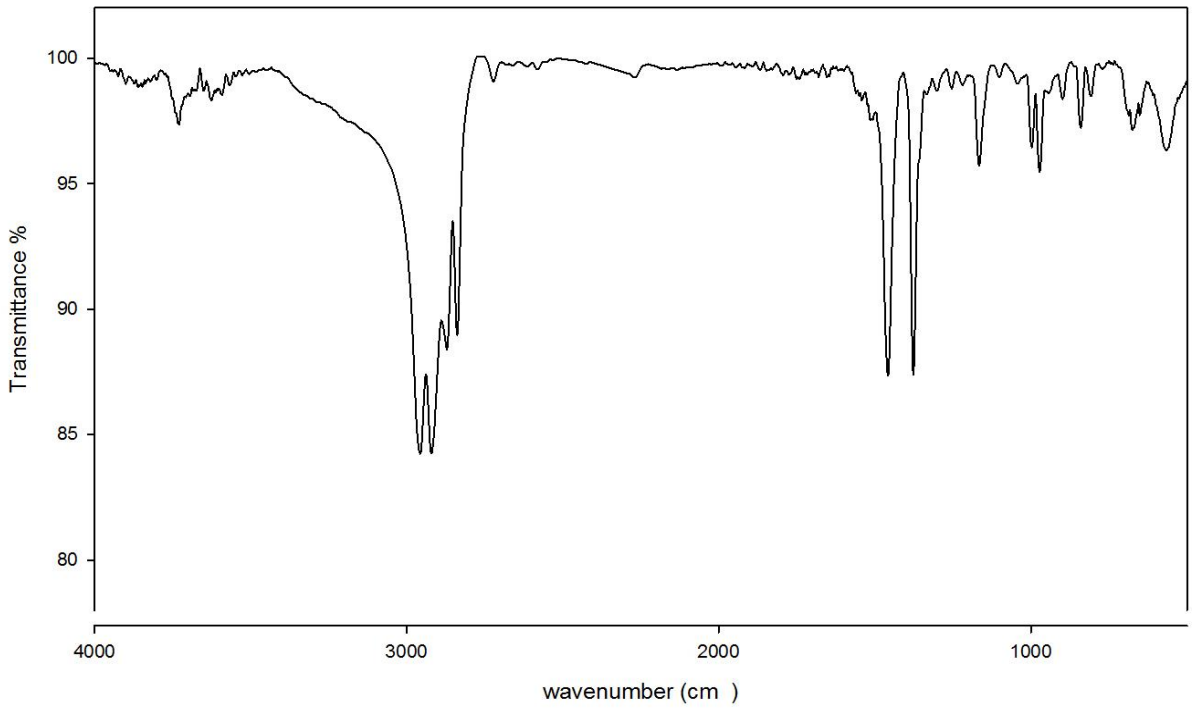

Figure 4 FTIR spectra of MAPP-a-MCNFs

Fig. 4 presents the FTIR spectrum of the maleic anhydride grafted polypropylene anchored magnetic cellulose nanofibrils (MAPP-a-MCNFs). The main peaks obtained were C-CH_3 stretching and CH_2 rocking vibrations at 840 cm^{-1}, C-C stretching and CH_3 rocking vibrations at 973 cm^{-1}, C-H bending and CH_2 wagging vibrations at 997 cm^{-1}, C-C stretching vibrations at 1163 cm^{-1}, CH_3 bending vibrations at 1379 cm^{-1}, C-H stretching vibration at 2980 cm^{-1}, C–H symmetrical deformation of CH_3 at 1370 cm^{-1} and β-glycosidic linkages between glucopyranose units at 1013 cm^{-1}.

Disappearance of band at 3448 cm^{-1} due to Fe-OH stretching vibration and O-H groups of carboxylated cellulose nanofibers, and band at 1635 cm^{-1} due to O-H deformation vibrations, clearly indicates the formation of chemical bonds between OH groups on the surface of Fe_3O_4 nanoparticles and COOH groups of carboxylated cellulose nanofibrils. The appearance of Si-O stretching vibration at 1024 cm^{-1}, carbonyl amide stretching vibration at 1715 cm^{-1}, C–N stretching vibration at 1375 cm^{-1}, and N–H stretching vibration (hydrogen bonded) at 2950 and 2925 cm^{-1} confirms the amidation between the maleic anhydride and amine group of silane-treated magnetic cellulose nanofibrils. Amide bond between maleic anhydride and silane-treated magnetic cellulose nanofibrils was provided the good distribution of magnetic cellulose in polymer matrix. The MA functional groups have been grafted to the head of

silane-treated magnetic cellulose nanofibrils, which allow them to be strongly bonded to the nanofibril surface and leave the PP tails behind.

4.2 Thermogravimetric Analysis

The TGA thermogram of carboxylated cellulose nanofibrils is shown in Fig. 5. Weight loss at about 100 ^{o}C (7.47%) is related to the removal of physisorbed water molecules from the surface of CCNFs. The inception decomposition temperature (Ti) and final decomposition temperature (Tf) of carboxylated cellulose nanofibrils are 232 and 386 °C respectively. Weight loss recorded is 72.32% which is attributed to the decomposition of organic structure of CCNFs. Carbonization of the residual products occurs over 386 °C. The higher thermal stability of CCNFs when compared to carboxylated cellulose is due to small particle size, high specific surface area and active surface groups.[30] The TGA thermogram of magnetic cellulose nanofibrils is shown in Fig. 6. The inception decomposition temperature (Ti) and final decomposition

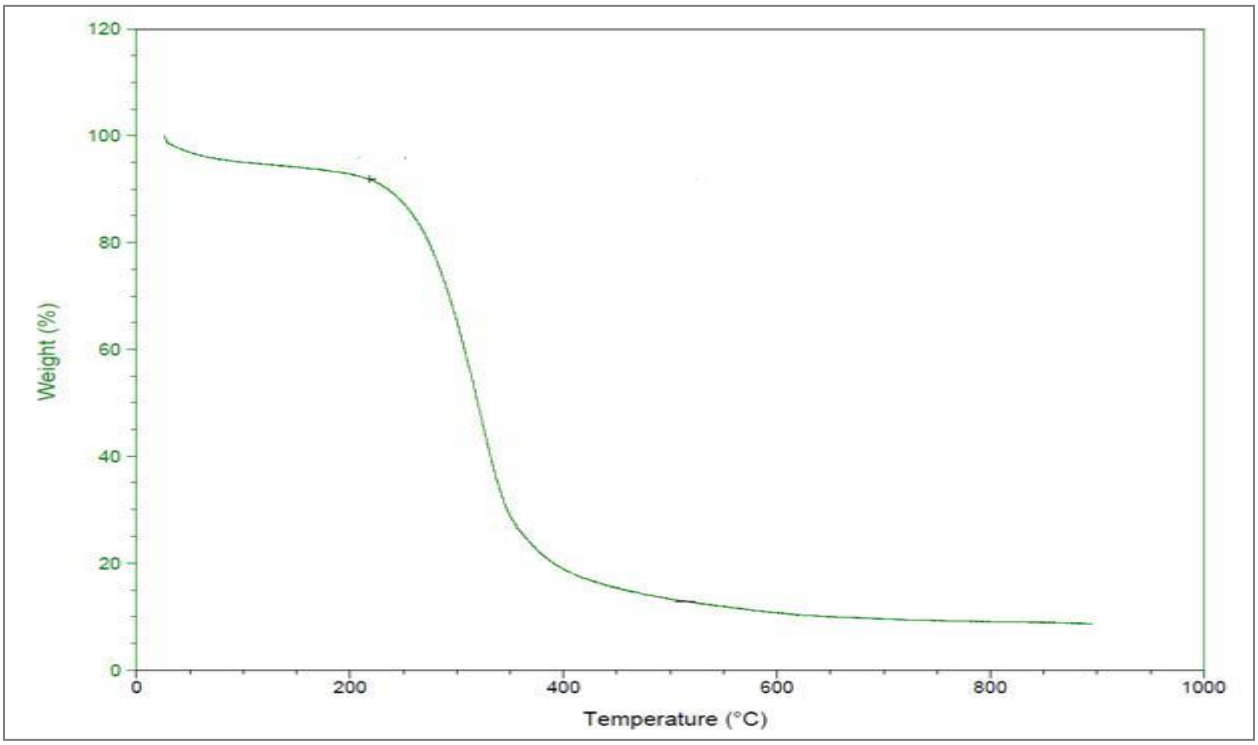

Figure 5 TGA of CCNFs

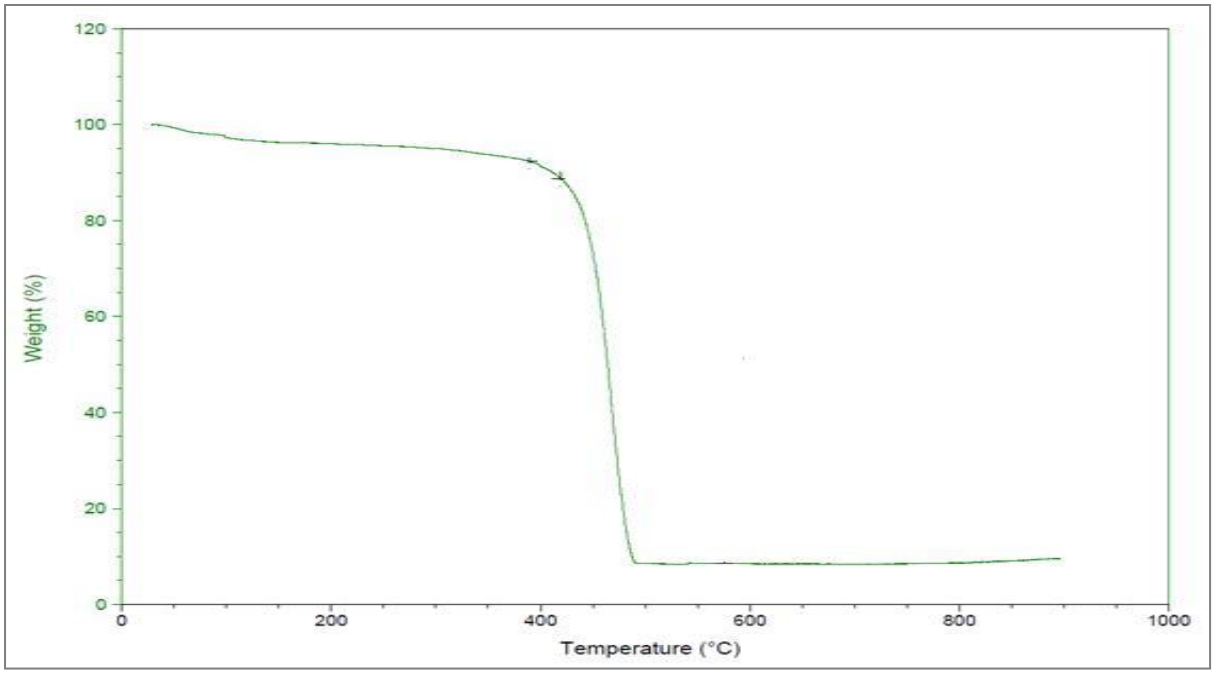

Figure 6 TGA of magnetic cellulose nanofibrils

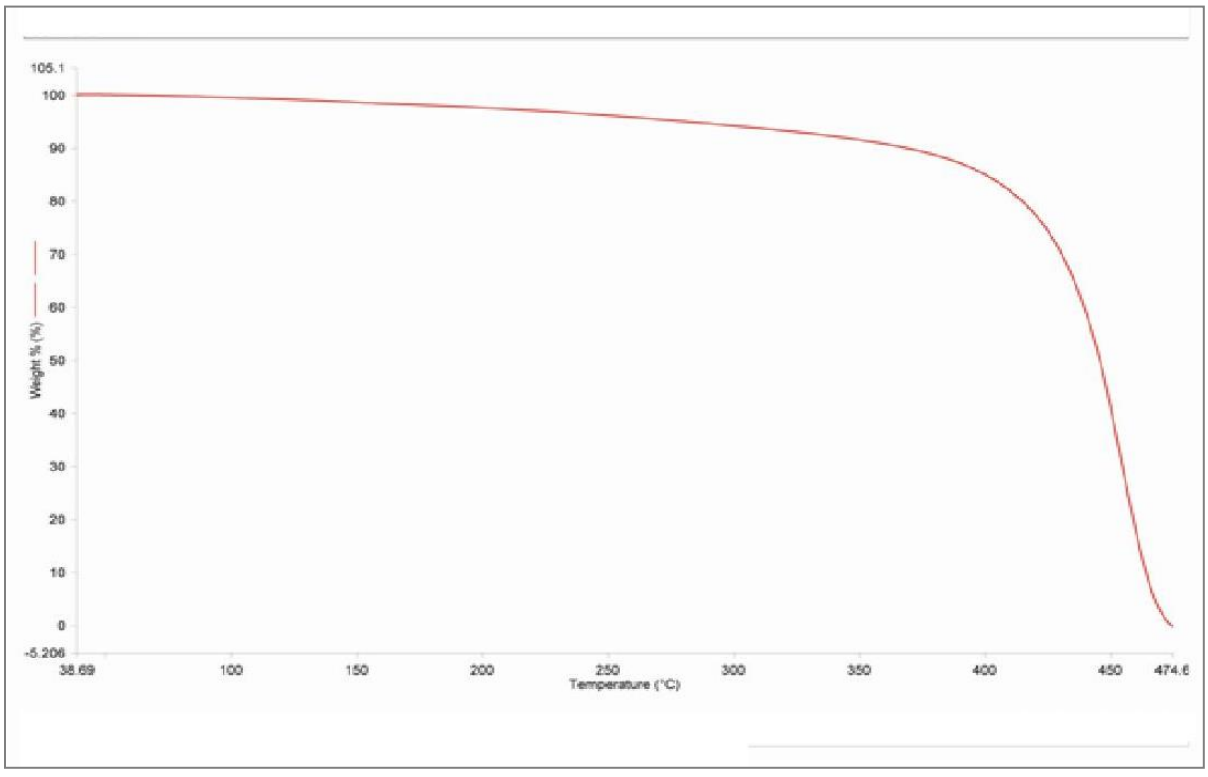

Figure 7 TGA of MAPP-a-MCNFs

temperature (Tf) of magnetic cellulose nanofibrils are 400 and 476°C respectively. The thermal decomposition of magnetic cellulose nanofibrils are shifted towards higher temperatures due to the strong adsorption of CCNFs on the surface of Fe_3O_4 NP. Also, Fe_3O_4 NP has barrier effect to slow down mass transport (volatilization) and thermal transport during decomposition of the CCNFs.

The (TGA) thermogram of maleic anhydride grafted polypropylene anchored magnetic cellulose nanofibrils (MAPP-a-MCNFs) is shown in Fig. 7. There are two stages of thermal degradation for maleic anhydride grafted polypropylene anchored magnetic cellulose nanofibrils. The first stage thermal degradation occurs in the range of 110-157^oC, due to the decomposition of un-reacted MA on the surface of silane-treated magnetic cellulose nanofibrils, with a weight loss upto 5.7%. From 400 ^oC to 474 ^oC, the second stage thermal degradation occurs, owing to the degradation of PP-g-MA/PP layer and decomposition of organic structure of CCNFs. After 474 ^oC, the TG curve is no longer falling, and the remaining part is Fe_2O_3 NP. Improvement in thermal stability for MAPP-a-MCNFs nanocomposites is due to the strong silane-treated magnetic cellulose nanofibrils -polymer interfacial interaction.

4.3 Scanning Electron Microscopy

The SEM micrograph of microcrystalline cellulose fibers is presented in Fig. 8. They show flat bands or ribbons with widths of 12–60 μm and had a smooth surface.

The morphology of carboxylated cellulose nanofibrils (CCNFs) shows a reduction in the width and the surface of fibers became rougher, indicating that ball milling has affected the structure (Fig. 9). This suggests that the mechanochemical treatment promotes the micronization of fibers into its constituent particles. After carboxylation, it seems that the ribbon-like shape was preserved and its size apparently decreased, with a width in the range of 20–100 nm and a length of 200–960 nm.

The SEM micrograph of the surfaces of Fe_3O_4 NP is presented in Fig. 10. They shows spherical shape morphology with average diameter of 45-50 nm, appears in the form of fractal aggregates, and forms an interconnected network structure due to magnetic dipole-dipole interactions and vander Waals forces among the NP.

The SEM image of Fe_3O_4-cellulose nanofibrils (Fig. 11) reveals near spherical morphology with homogeneous dispersion of Fe_3O_4, NP within the CCNFs matrix of a diameter of 75-80 nm.

The SEM micrograph of the surfaces of maleic anhydride grafted polypropylene anchored magnetic cellulose nanofibrils (MAPP-a-MCNFs) is presented in Fig. 12. It shows granular morphology with homogeneous dispersion of silane-treated magnetic cellulose nanofibrils within the PP matrices by magnetic dipole forces.

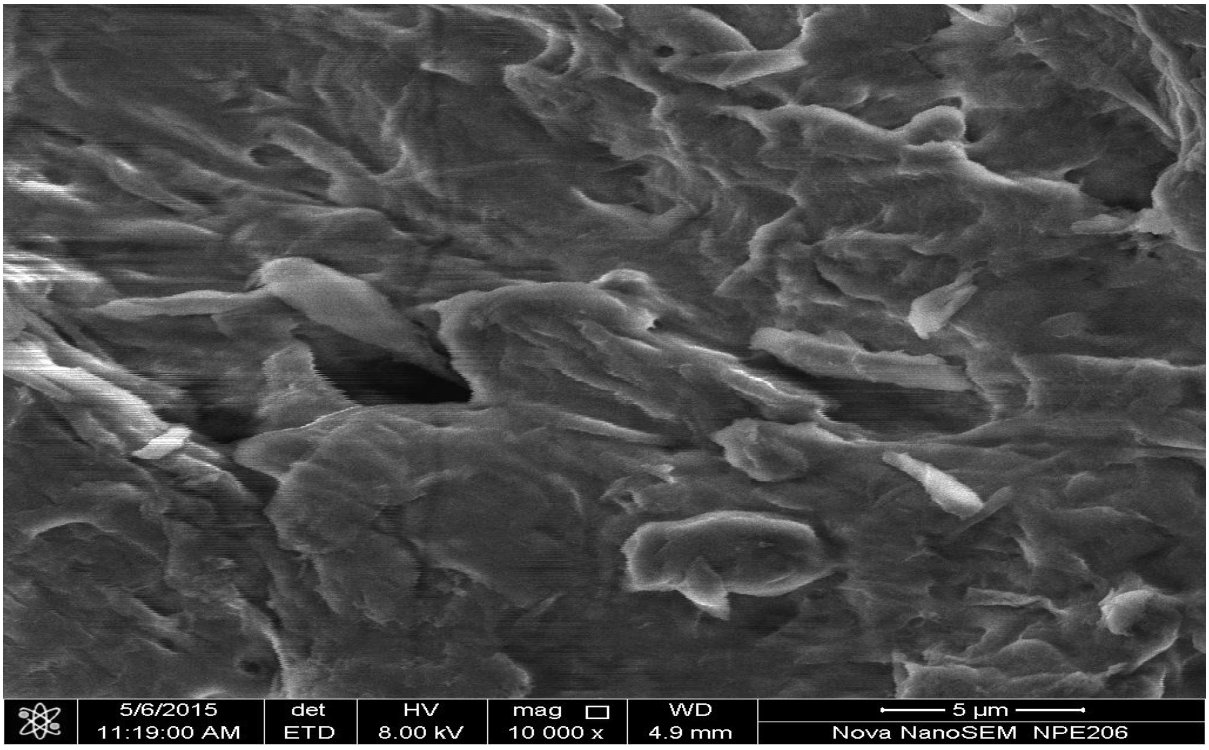

Figure 8 SEM of microcrystalline cellulose fibers

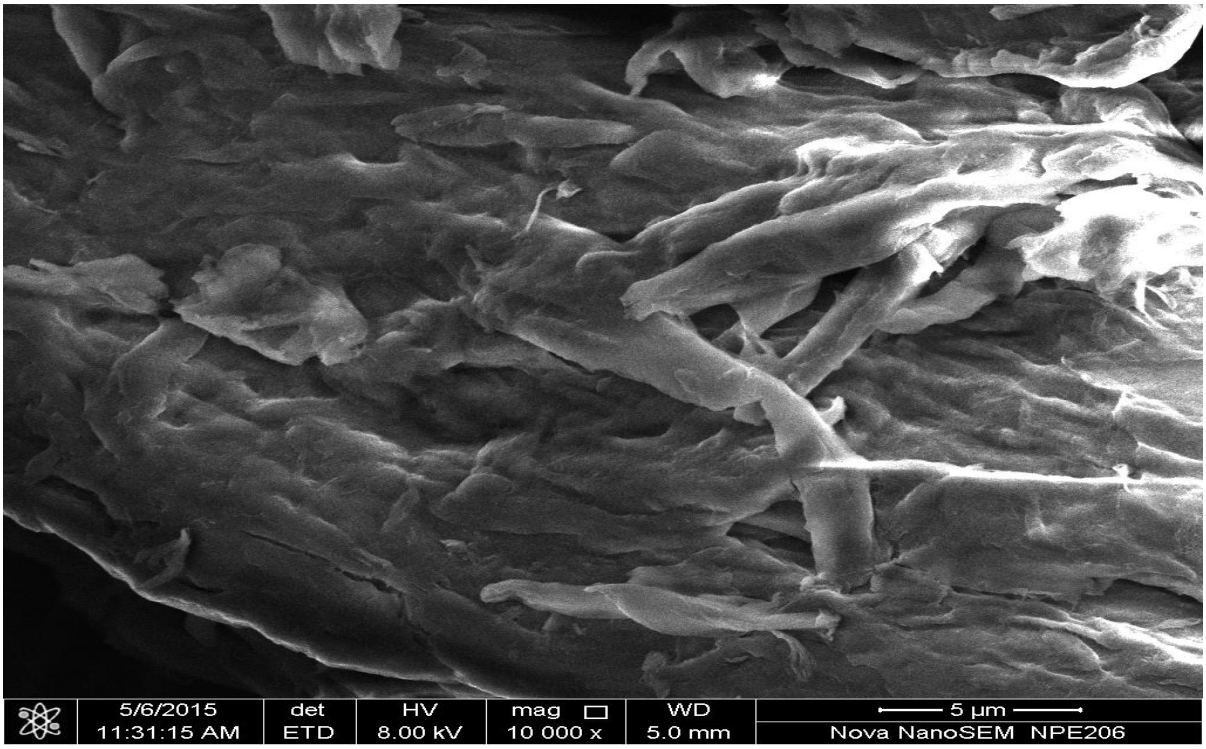

Figure 9 SEM of carboxylated cellulose nanofibrils

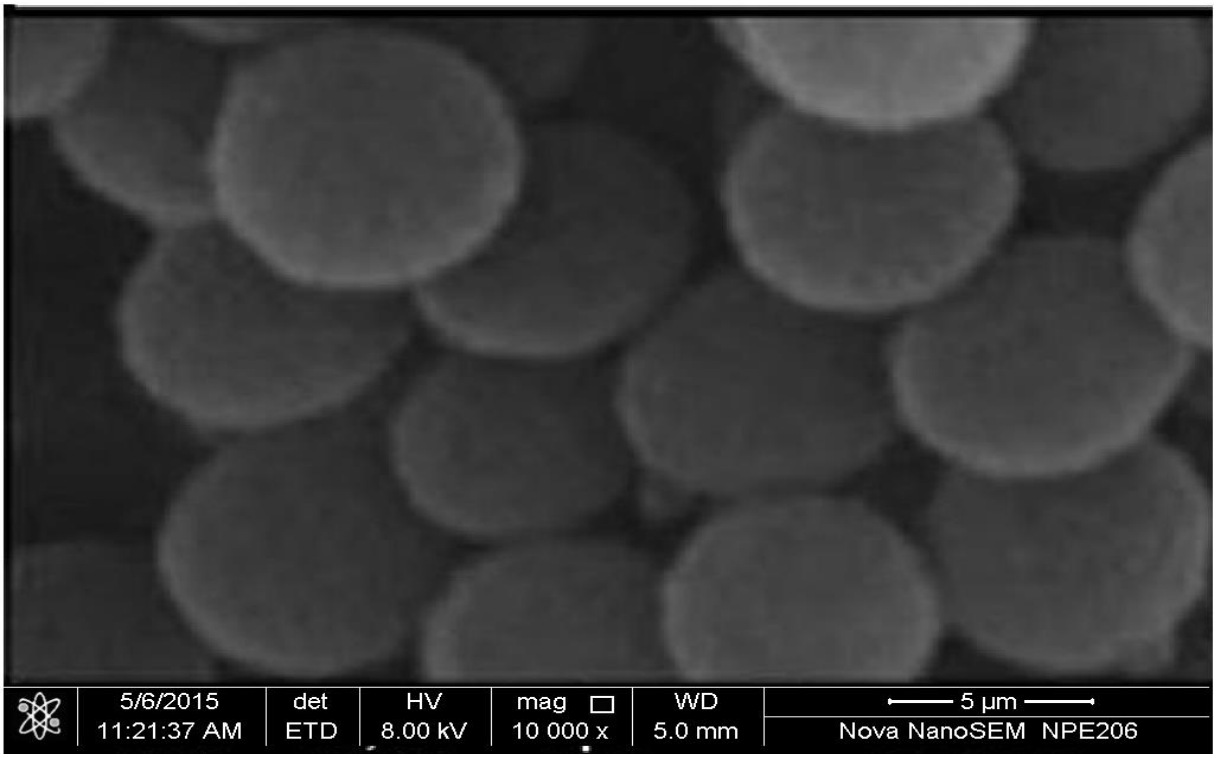

Figure 10 SEM of Fe_3O_4 nanoparticles

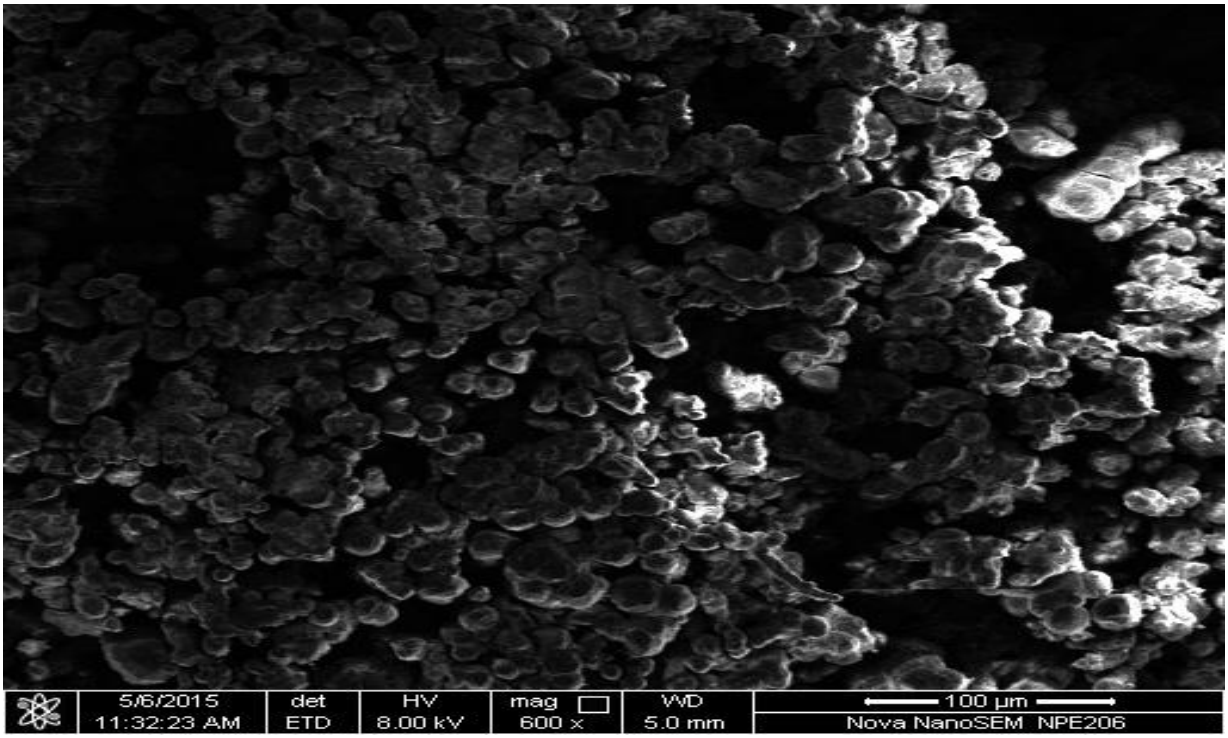

Figure 11 SEM of Fe_3O_4-cellulose nanofibrils

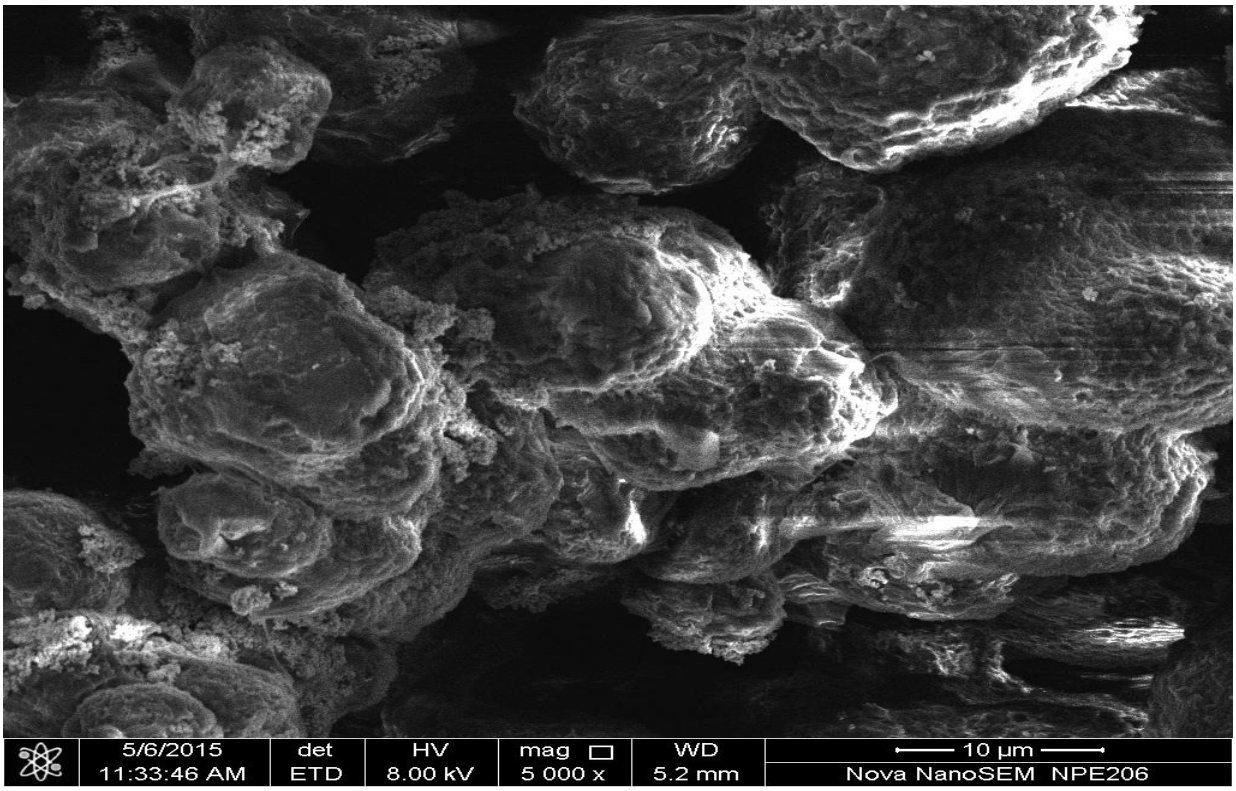

Figure 12 SEM of MAPP-a-MCNFs nanocomposites

4.4 Oil Absorption Capacity

Fig. 13 shows the results of sorption times (5- 30 min) on heavy crude oil removal and as expected, sorption capacity of maleic anhydride grafted polypropylene anchored magnetic cellulose nanocomposites (MAPP-a-MCNFs/PP) increases with increase of time and reaches the maximum at 15 min. remains constant for both 1 DWO (Day Weathered Oil) and 7 DWO. This may be due to adsorption of oil on the surface of PP first and then penetrate to the pores of PP and walls of cellulose nanofibrils respectively. Sorption capacity of 7 DWO is less than 1 DWO due to the increase of viscosity of crude oil by "weathering". The MAPP-a-MCNFs/PP nanocomposites never absorb water because the magnetic cellulose nanofibril is completely coated with water repellent silane and isotactic polypropylene. These nanocomposites never undergoes increase in specific gravity and can be always kept floating on water surface. The MAPP-a-MCNFs/PP nanocomposites has higher buoyancy than the polypropylene, and can be kept floating on water surface for a longer period of time. Further, the MAPP-a-MCNFs/PP nanocomposites is prevented from decaying by such polypropylene coating.

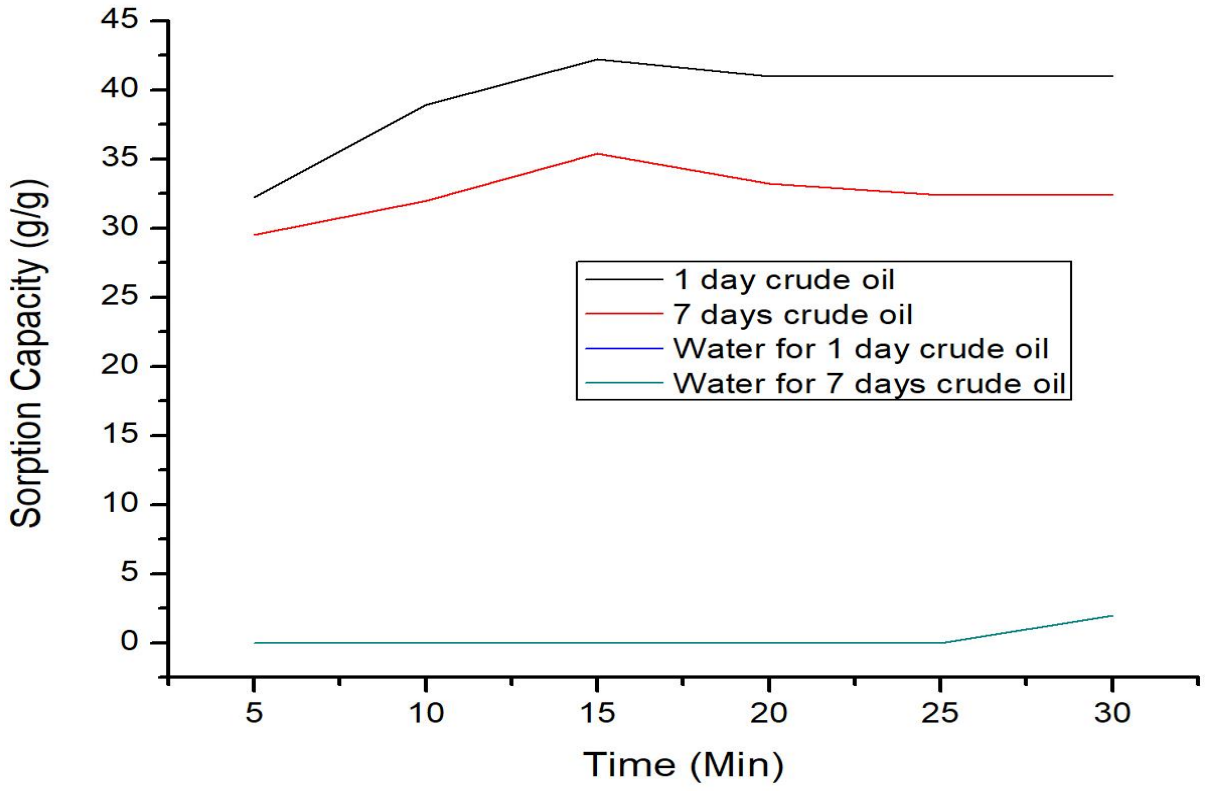

Figure 13 Effect of time on oil sorption capacity

5. CONCLUSION

Maleic anhydride grafted polypropylene anchored magnetic cellulose nanofibrils (MAPP-a-MCNFs) were fabricated through amidation of silane-treated magnetic cellulose nanofibrils and MAPP. Evidence of chemical interaction between silane-treated magnetic cellulose nanofibrils and MAPP has been obtained by FTIR, TGA and SEM analysis. The porous nanocomposites not only exhibited interesting superhydrophobicity, but also fast and selectively removed crude oil from water surface under magnetic field. Because of their good corrosion resistance, unsinkable property, environmental friendliness, and easy operation, these MAPP-a-MCNFs/PP nanocomposites might be a kind of promising absorbent materials for removing oils from water surface.

6. REFERENCES

1. Kingston, P.F, "*Long-term environmental impact of oil spills*", Spill Science and Technology Bulletin 2002; 7: 53-61.
2. Annunciado, T.R, Sydenstricker, T.H.D, Amico, S.C, "*Experimental investigation of various vegetable fibers as sorbent materials for oil spills*", Marine Pollution Bulletin 2005; 50(11): 1340-1346.
3. Karan, C.P, Rengasamy, R.S, Das, D, "*Oil spill clean-up by structured fiber assembly*", Indian Journal of Fibre & Textile Research 2011; 36: 190-200.
4. Payne, J.R, Phillips, C.R, "*Photochemistry of petroleum*", Environmental Science & Technology 1985; 19(7): 569-579.
5. Jordan, R.E, Payne, J.R, "*Fate and weathering of petroleum spills in the marine environment: A literature review and synopsis*", Ann Arbor science publishers, Ann Arbor, MI, USA. 1980.
6. Sang, R.C, "*Cereal Straw as a Resource for Sustainable Biomaterials and Biofuels*", First ed. Elsevier, UK. 2010.
7. Chang, S.E, Stone, J, Demes, K, "*Consequences of oil spills: a review and framework for informing planning*", Ecology and Society 2014; https://doi.org/10.5751/ES06406-190226.
8. Wardley Smith, J, "*The control of oil pollution*", Graham and Trotman Publication, London. 1983.
9. Leung, M, "*Bioremediation: Techniques for cleaning up a mess*", Journal of Biotechnology 2004; 2: 18-22.

10. Al-Majed, A.A, Adebayo, A.R, Hossain, M.E, "*A sustainable approach to oil spills*". Journal Environmental Management 2012; 113: 213-227.
11. Ceylan, D., Dogu, S, Karacik, B, Yakan, S.D, Okay, O.S, Okay, O, "*Evaluation of butyl rubber as sorbent material for the removal of oil and polycyclic aromatic hydrocarbons from seawater*", Environmental Science & Technology 2009; 43: 3846-3852.
12. Payne, K.C, Jackson, C.D, Aizpurua, C.E, Rojas, O.J, Hubbe, M.A, "Oil spills abatement: factors affecting oil uptake by cellulosic", Environmental Science & Technology 2012; 46: 7725-7730.
13. Tewari, S, Sirvaiya, A, "*Oil spill remediation and its regulation*", International Journal of Research in Science & Engineering 2015; 1(6): 1-7.
14. Yao, X, Song, Y, Jiang, L, "*Applications of bio-inspired special wettable surfaces*", Advanced Materials 2011; 23(6), 719-734.
15. Feng, L, Zhang, Z, Mai, Z, Ma, Y, Liu, B, Jiang L, Zhu, D, "*A super-hydrophobic and super-oleophilic coating mesh film for the separation of oil and water*", Angewandte Chemie International Edition 2004; 43(15), 2012-2014.
16. Feng, X.J, Jiang, L, "*Design and Creation of Superwetting/Antiwetting Surfaces*", Advanced Materials 2006; 18(23), 3063-3078.
17. Su, C, "*Highly hydrophobic and oleophilic foam for selective absorption*", Applied Surface Science 2009; 256(5), 1413-1418.
18. Wang, C, Yao, T, Wu, J, Ma, C, Fan, Z, Wang, Z, Cheng, Y, Lin, Q, Yang, B, *"Facile approach in fabricating superhydrophobic and superoleophilic surface for water and oil mixture separation",* ACS Applied Materials & Interfaces, 2009; 1(11), 2613-2617.
19. Chu, Y, Pan, Q, "*Three-dimensionally macroporous Fe/C nanocomposites as highly selective oil-absorption materials*", ACS Applied Materials Interfaces 2012; 4, 2420-2425.
20. Qing Zhu, Feng Tao, Qinmin Pan, "*Fast and Selective Removal of Oils from Water Surface via Highly Hydrophobic Core−Shell Fe_2O_3@C Nanoparticles under Magnetic Field*", ACS Applied Materials Interfaces 2010; 2(11), 3141-3146.
21. Ting Lü, Yi Chen, Dongming Qi, Zhihai Cao, Dong Zhang, Hongting Zhao, "Treatment of emulsified oil wastewaters by using chitosan grafted magnetic nanoparticles", Journal of Alloys and Compounds 2017; 696, 1205-1212.

22. Yu, L.H, Hao, G.Z, Gu, J.J, Zhou, S, Jiang, W, "*Fe_3O_4/PS magnetic nanoparticles: synthesis, characterization and their application as sorbents of oil from waste water*", Journal of Magnetism and Magnetic Materials 2015; 394, 14-21.
23. Song, B.T, Zhu, J, Fan, H.M, "*Magnetic fibrous sorbent for remote and efficient oil adsorption*", Marine Pollution Bulletin 2017; 120, 159-164.
24. Gui, X.L, Zeng, Z.P, Lin, Z.Q, Gan, Q.M, Xiang, R, Zhu, Y, *"Magnetic and highly recyclable macro porous carbon nanotubes for spilled oil sorption and separation*", ACS Applied Materials Interfaces 2013; 5, 5845-5850.
25. Silviana, S, Hadiyanto, H, "*Preparation of sago starch-based biocomposite reinforced microfibrillated cellulose of bamboo assisted by mechanical treatment*", AIP Conference Proceeding on Green Process, Material, and Energy: A Sustainable Solution for Climate Change 2017; 1855, 030024-1–030024-5; doi: 10.1063/1.4985494.
26. Xie, W, Ma, N, "*Immobilized lipase on Fe_3O_4 nanoparticles as biocatalyst for biodiesel production*", Energy & Fuels 2009; 23, 1347-1353.
27. Fujisawa, S, Okita, Y, Fukuzumi, H, Saito, T, Isogai, A, "*Preparation and characterization of TEMPO-oxidized cellulose nanofibril films with free carboxyl groups"*, Carbohydrate Polymers 2011; 84, 579–583.
28. Durdureanu-Angjeluta, A, Ardeleanua, R, Pintealaa, M, Harabagiua, V, Chiracc, H, Simionescua, B.C, "*Silane covered magnetic particles: Preparation and characterization*", Digest Journal of nanomaterials and biostructures 2008; 3, 33-40.
29. Sachin N. Sathe, Srinivasa Rao, G.S, Surekha Dev, "*Grafting of Maleic Anhydride onto Polypropylene: Synthesis and Characterization*", Journal of Applied Polymer Science 1994; 53, 239-245.
30. Miao Cheng, Zongyi Qin, Yannan Liu, Yunfeng Qin, Tao Li, Long Chen, Meifang Zhua, *"Efficient extraction of carboxylated spherical cellulose nanocrystals with narrow distribution through hydrolysis of lyocell fibers by using ammonium persulfate as an oxidant"*, Journal of Material Chemistry A, 2014; 2, 251-258.